Catalysis Letters (2018) 148:1879–1892
https://doi.org/10.1007/s10562-018-2399-z

Functionalized Hydrotalcite Tethered Ruthenium Catalyst for Carbon Sequestration Reaction

Vivek Srivastava[1]

Received: 23 January 2018 / Accepted: 29 April 2018 / Published online: 11 May 2018

Abstract
We successfully synthesized a series of hydrotalcite functionalized Ru metal catalytic system. Sophisticated analytical techniques like FTIR, N_2 physisorption, ICP-OES, XPS and TEM analysis were applies to understand the physiochemical nature of and structural arrangements of functionalized hydrotalcite materials. We applied this system with and without ionic liquid medium and Schiff-base-modified Ru nanometal catalyst were found highly active in terms of formic acid synthesis. As per the spectral analysis activation of CO_2 was confirmed by a weakly bonded carbamate zwitterion intermediate followed by simple addition of Lewis base adduct of CO_2 gas. We also recycled the ionic liquid mediated Ru metal loaded functionalized hydrotalcite system up to eight runs without any significant loss of catalytic activity.

Graphical Abstract

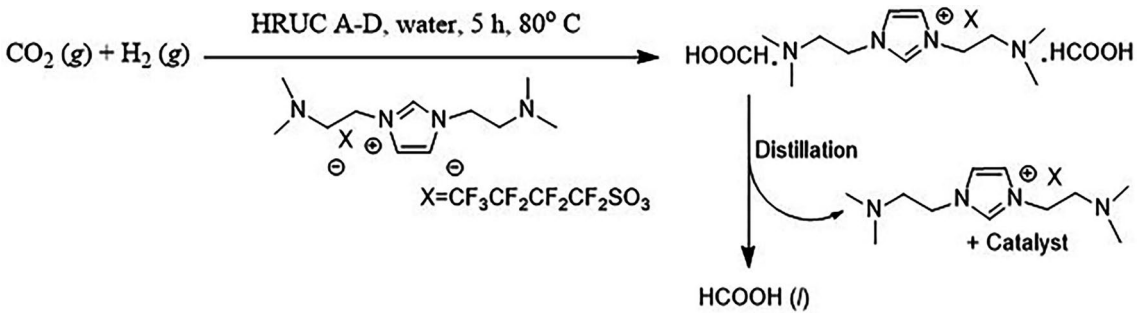

Keywords Hydrogenation · Hydrotalcite · Ru catalytic system · Carbon dioxide · Formic acid

1 Introduction

The reduction of CO_2 emission into the atmosphere is a serious requirement as it is considered as an important part of greenhouse gases. Apart from CO_2 storage such as fixation in carbonates, conversion of CO_2 gas to important platform chemicals, not only provides an alternative to capture the CO_2 gas but also utilize CO_2 as cheap C1 source [1, 2]. Among the numerous hydrogenation products of CO_2 gas, formic acid, is considered as a most striking chemical because of its straight as a feedstock chemical, leather, rubber, fragrance and hydrogen source for fuel cells. In addition, the hydrogenation of CO_2 gas to formic acid also open area where other chemicals like methanol and methane can also be synthesized using same reaction pathway [1–3]. However, easy and complete CO_2 reduction is still a task for the scientific community due to the extreme thermodynamic stability of CO_2 molecule.

Many reports have been published to utilize the application of homogenous as well as heterogenous catalysts with and without additives to hydrogenate CO_2 gas to formic acid [4, 5]. The main obstacle to achieve selective and easy hydrogenation of CO_2 is the positive standard free energy

✉ Vivek Srivastava
vivek.shrivastava@niituniversity.in

[1] Basic Sciences: Chemistry, NIIT University, NH-8 Jaipur/Delhi Highway, Neemrana, Rajasthan 301705, USA

of the hydrogenation reaction. A series of supported and unsupported transition metal complexes or nanocatalysts were utilized with and without base to achieve reasonable conversion of CO_2 to formic acid [6, 7]. Nevertheless, the easy recovery of formic acid and catalyst recycling as well as requirement of base as an additive are still a challenge for scientific community. This problem also considered as the main shortcomings for the industrialization of CO_2 hydrogenation reaction [7, 8].

Hydrotalcite clay (HTc) is a naturally occurring materials having layered double hydroxide (LDH) structure [9, 10]. The general formula of hydrotalcite material is $[M_{1-x}^{2+} M_x^{3+} (OH)_2]^{x+} (A^{n-})_{x/n} \cdot mH_2O$, where A^- are anions like CO_3^{2-}, OH^-, Cl^- or SO_4^{2-}. The morphology of natural and synthetic HTc are similar to brucite clay but their basicity varies with the concentration of cations [9–12]. Such variation makes the HTc more interesting in terms of the catalyst as well as catalyst support [13, 14]. HTc is very attractive systems due to their striking physiochemical properties that can be modified by a suitable choice of the metal ions or functional guest anions [11, 12]. Therefore, HTc materials have been effectively applied in numerous areas such as adsorption materials for gases (CO_2, H_2S, and SO_2), precursors for functional materials, photochemistry and electrochemistry. In addition, the presence of hydroxyl groups makes the HTc as an active and recyclable solid base catalyst for the variety of organic reaction. In recent years the applications of HTc have been increased not only as heterogeneous catalyst and catalyst support but also as anion exchanger, CO_2 absorbent and in water treatment [15, 16]. As catalyst support, HTs have been used to immobilize various transition metal nanoparticles and homogeneous catalysts [16, 17]. Alkoxysilane linkage is one of the easiest ways to link homogeneous or heterogeneous catalyst over hydrotalcite surface. Surprisingly, anchoring the homogeneous or heterogeneous catalysts over silica and alumina is well studied but still very few reports are available with respect to alkoxysilane interaction with hydrotalcite clay.

In this report, we are offering the synthesis of hydrotalcite tethered Ru metal catalyst (HRUC) for the hydrogenation of CO_2 gas in the functionalized ionic liquid medium. The HRUC catalytic system was synthesized by a multistep grafting process using iminophosphine ligand tethered to hydrotalcite inorganic support.

2 Experimental

Reagent Plus® grade chemicals were purchased from Sigma Aldrich and other chemical suppliers. FTIR measurements were conducted with Bruker Tensor 27 in DRIFT mode (KBr powder) with a scanning range 400–4000 cm^{-1}. Perkin Elmer Optima 3300 XL ICP-OES was used to study the elemental analysis. Nuclear Magnetic Resonance (NMR) spectra were recorded on a standard Bruker 300WB spectrometer with an Avance console at 400 and 100 MHz for ^1H NMR. The morphology of catalysts was investigated by transmission electron microscopy (TEM) using a Philips CM12 instrument. Kratos-Axis 165 with Mg Kα radiation 1254 eV was used to perform X-ray photoelectron spectroscopy (XPS). DTA–TGA thermal analyzer apparatus (Shimadzu DTG-60H) was used to study the thermal stability of an ionic liquid. BET surface area, pore size, and pore volume measurements of the catalysts were determined from a physical adsorption of N_2 using liquid nitrogen by an ASAP2420 Micromeritics adsorption analyzer (Micromeritics Instruments Inc). All the samples were degaussed at the 250 °C for 2 h earlier before going to the measurements to make moisture free catalysts surface and pore. The surface area and pore size distribution (PSD) were measured from the BET and BJH equations, respectively, by the instrument software. All the hydrogenation reactions were carried out in a 100-mL stainless steel autoclave (Amar Equipment, India).

2.1 Synthesis of Hydrotalcite Material

The hydrotalcite with Mg and Al species was synthesized using coprecipitation method [13]. An aqueous solution containing $Mg(NO_3)_2 \cdot 6H_2O$ (80.0 g) and $Al(NO_3)_3 \cdot 9H_2O$ (37.74 g) in 225 ml of water (*solution A*) was prepared (*while maintaining an Mg/Al molar ratio of 3*). A separate *solution B*, containing NaOH (54 g) and Na_2CO_3 (21.6 g) in 675 ml of water was prepared separately. *Solution A* and *B* were simultaneously added dropwise into distilled water under vigorous mechanical stirring with maintaining the pH of the resulting solution in the range of 9.5–10 at 55 °C temperature. The slurry was ripened for 30 min under forceful stirring at 55 °C and was allowed to stand in its mother liquor for 3 h. The precipitate was washed several times until a pH of 7 was reached and was then dried at 110 °C for 12 h. The calcined hydrotalcite (HT) was obtained by calcining the hydrotalcite (HTc) at 600 °C for 4 h.

2.2 Synthesis of Iminophosphine Ligands-*Moiety A* and Iminophosphine Ligands with Ru Metal-Ru-*Moiety A*

A perfectly dried 100 ml round bottom flask was charged with 2-(diphenylphosphine) benzaldehyde (2.5 mmol) and 1-propylamine (10 mL). All reactants were refluxed under nitrogen for 5 h to obtain the Schiff-base. After cooling the reaction mass to room temperature, monophosphate ligand was isolated as red–brown oil after vacuum distillation and column chromatography (yield 91%).

^1H NMR (400 MHz, CD_2Cl_2): δ = 9.02 (s, 1H), 8.04 (s, 1H), 7.44–7.31 (m, 12 H), 6.97 (s, 1 H), 3.42 (t,

2 H), 1.57–1.53 (q, 2 H), 0.82–0.77 (t, 3 H); ^{13}C NMR (100 MHz, CD_2Cl_2): δ = 160.02, 134.25, 128.73, 63.34, 23.95, 11.79 ppm. ^{31}P NMR: (300 MHz, CD_2Cl_2, ppm) δ = − 13.02 ppm.

Ru-Moiety-A was obtained by reacting moiety-A (2 g) with $RuCl_3{\cdot}3H_2O$ (2.1 g) in dry ethanol (25 mL) under an inert atmosphere. The combined reaction mass was refluxed for 12 h. After cooling the reaction mass was washed with dry ethanol (10 × 2 mL) under a nitrogen atmosphere. Perfectly dried material (*Ru-Moiety-A*) through lyophilizer was kept under nitrogen atmosphere.

2.3 Synthesis of Alkoxysilane-*Moiety B*

A perfectly dried 100 mL round bottom flask was charged with 2-(Diphenylphosphino) benzaldehyde (0.75 g), 3-(Trimethoxysilyl)propylamine (0.375 g) and 40 mL dry THF under a nitrogen atmosphere. The combined reaction mass was allowed to stir at 100 °C for 5 h. after completion the reaction, we obtained alkoxysilane compound with bidentate iminophosphine ligand as a yellow oily liquid (after the careful removal of solvent and volatile impurities followed by vacuum distillation and column chromatography) (yield 95%).

^{1}H NMR (400 MHz, CD_2Cl_2): δ = 8.9 (s, 1H), 8.03 (s, 1H), 7.45–7.28 (m, 12 H), 6.93 (s, 1 H), 3.52 (s, 9 H), 3.47 (m, 2 H), 1.68–1.61 (m, 2 H), 0.58–0.51 (m, 2 H); ^{13}C NMR (100 MHz, CD_2Cl_2): δ = 158.58, 134.15, 128.78, 65.15, 50.80, 24.61, 8.74 ppm.; ^{31}P NMR: (300 MHz, CD_2Cl_2, ppm) δ = − 13.05 ppm.

2.4 Synthesis of Phosphine Functionalized Calcined Hydrotalcite *(ABIL-HT-A to C)*

Post-synthetic grafting method was applied to obtain phosphine functionalized calcined hydrotalcite material under an inert atmosphere. Phosphine ligand (2 mmol) was allowed to react with calcined hydrotalcite (1 g) in dry toluene under (20 mL) nitrogen atmosphere. The reaction mass was stirred for next 24 h at room temperature (30–35 °C). The resulting solid mass was washed several times to dry toluene (10 × 2 mL). The recovered solid was carefully dried in a lyophilizer. The perfectly dried pale-yellow solid (ABIL-HT-A to C) was carefully placed under vacuum at room temperature (yield 98%).

2.5 Synthesis of Amine Functionalized Calcined Hydrotalcite *(ABIL-HT-D)*

Calcined hydrotalcite (1 g) was mixed with 3-aminopropyltrimethoxysilane (1.2 mmol) in dry toluene (20 mL). The combined reaction mass was heated and vigorously stirred at room temperature (30–35 °C) for next 24 h under nitrogen atmosphere. The resulting solid material was perfectly washed and filtered with dry toluene. (10 × 2 mL) and then the solid was dried in a lyophilizer. Light yellow solid (ABIL-HT-D) was sensibly stored under vacuum in a nitrogen atmosphere (Yield 98%).

2.6 Synthesis of Ru-Tethered Pre-catalyst (HRUC-A to D)

The ABIL-HT-A to D was added to $RuCl_3{\cdot}3H_2O$ in anhydrous ethanol (25 mL) under nitrogen by keeping the ratio of Ru and phosphorus (1:1). The resulting reaction mixture was refluxed for 10 h. After cooling the reaction mass, the resulting solid material was carefully washed several times with dry ethanol (10 × 2 mL) under a nitrogen atmosphere. The recovered black solid was dried using lyophilizer and further carefully stored under inert atmosphere (yield 98%).

2.7 CO_2 Hydrogenation Reaction and Recycling Experiment

After performing the catalysts pretreatment process at 45 °C for 20 min under 10 MPa pressure of hydrogen gas, all the gases were completely replaced with nitrogen gas at room temperature. Then all the reactants (except H_2 and CO_2 gas) were added along with a known quantity of dioxane (internal standard for ^{1}HNMR analysis) to the reaction vessel (as per Tables 1, 2) without opening the autoclave. Then nitrogen gas was completely replaced by CO_2 gas (by 2–3 times flushing). Absorption of CO_2 gas was carried out at 80 °C with 20 bar pressures for 1 h. Later, after reducing the temperature of the autoclave to 40 °C, hydrogen gas was added into the reactor. The combined reaction mass was allowed at per Tables 1 and 2. The combined reaction mass was permitted to cool at room temperature before opening the reaction vessel. The small quantity of crude reaction mass was used for ^{1}HNMR analysis and titration to quantify the amount of formic acid in the reaction sample. It is important to notice here that no sign of ionic liquid, as well as dioxane decomposition, was recorded during ^{1}H NMR analysis. The result attained from ^{1}H NMR analysis were found in good agreement with titration method. Recovery of formic acid was carried out easily under reduced pressure. At 50 °C, initially, all the water and other volatile impurities were removed the at 75–80 °C, under nitrogen flow the formic acid was isolated.

2.7.1 Catalyst Recycling with Ionic Liquid

After careful isolation of formic acid, ionic liquid immobilized catalytic system was washed several times with dry diethyl ether (5 × 2 mL) to remove all the organic impurities and further dried in a lyophilizer. The perfectly dried ionic

Table 1 CO_2 hydrogenation reaction optimization and result

Entry	Catalyst (0.1 g + 5 mL water + 2 mL EtN_3)	P (H_2) (P_{total}) (MPa)	T °C	t (h)	TON (mol_{FA}/mol_{Ru})[a]	TON ($mol_{FA}/mol_{Ru} \times h^{-1}$)
1.	None	20 (40)	80	5	–	–
2.	$RuCl_3 \cdot 3H_2O$	20 (40)	80	5	12.17	2.4
3.	$RuCl_3$/calcined hydrotlcite	20 (40)	80	5	38.04	7.6
4.	HRUC-A	20 (40)	80	5	1275.85	255.2
5.	HRUC-B	20 (40)	80	5	601.87	120.4
6.	HRUC-C	20 (40)	80	5	766.14	153.2
7.	HRUC-D	20 (40)	80	5	891.81	178.4
8.	HRUC-A	30 (60)	80	5	1268.22	253.6
9.	HRUC-A	15 (30)	80	5	609.96	122
10.	HRUC-A	20 (40)	120	5	1271.87	254.4
11.	HRUC-A	20 (40)	60	5	1013.34	202.7
12.	HRUC-A	20 (40)	80	2	917.82	458.9
13.	HRUC-A (0.05 g)	20 (40)	80	2	561.81	280.9
14.	HRUC-A (0.15 g)	20 (40)	80	2	1278.71	639.4
15.	HRUC-A	20 (40)	80	7	1273.02	181.9
16.	Moiety-A	20 (40)	80	5	56.41	11.3
17.	$RuCl_2$ $(PPh_3)_3$	20 (40)	80	5	175.91	35.2

[a]*FA* formic acid

Table 2 Reaction optimization of Ionic liquid mediated HRUC-A catalyzed CO_2 hydrogenation

Entry[a]	T (°C)	Water (mL)	P (H_2) (P_{total}) (MPa)	Time (h)	HCOOH/IL	TON (mol_{FA}/mol_{Ru})	TON ($mol_{FA}/mol_{Ru} \times h^{-1}$)
1.	80	0	20 (40)	5	0.14	781.21	156.2
2.	80	1	20 (40)	5	0.29	845.13	169.0
3.	80	2	20 (40)	5	0.81	1011.91	202.4
4.	80	3	20 (40)	5	0.97	1217.58	243.5
5.	80	4	20 (40)	5	1.21	1319.68	263.9
6.	80	5	20 (40)	5	1.81	1571.62	314.3
7.	80	6	20 (40)	5	1.84	1574.53	314.9
8.	100	5	20 (40)	5	1.85	1581.62	313.4
9.	80	5	20 (40)	2	0.29	791.01	395.5
10.	80	5	20 (40)	6	1.95	1579.91	263.3
11.	80	5	20 (40)	8	1.95	1580.97	197.6
12.	80	5	20 (40)	10	2.1	1578.93	157.9
13.	60	5	20 (40)	5	0.38	1231.17	246.2
14.	80	5	30 (60)	5	1.81	1586.94	317.4
15.	80	5	10(20)	5	0.42	721	144.2
16.[b]	80	5	20 (40)	5	0.17	317.62	63.5
17.[c]	80	5	20 (40)	5	1.98	1572.37	314.5
18.[d]	80	5	20 (40)	5	0.84	1038.10	207.6

[a][DAMI][$CF_3CF_2CF_2CF_2SO_3$] ionic liquid (0.150 g) + HRUC-A (0.1 g)

[b][bmim][NTf_2] (0. 150 mL) + HRUC-A (0.1 g)

[c][DAMI][$CF_3CF_2CF_2CF_2SO_3$] ionic liquid (0.250 g) + HRUC-A (0.1 g)

[d][DAMI][$CF_3CF_2CF_2CF_2SO_3$] ionic liquid (0.50 g) + HRUC-A (0.1 g)

liquid immobilized catalytic system was again pretreated at 45 °C for 20 min under 10 MPa pressure of hydrogen gas, before going to next recycling for CO_2 hydrogenation.

2.7.2 Catalyst Recycling Without Ionic Liquid

After successful isolation of formic acid, the catalytic system was washed several times with ether to remove all the organic impurities from the catalysts and then the catalyst was dried in a lyophilizer. The fresh catalyst was added to the used catalyst, in case if any catalysts loss is there during the workup process. After adjusting the quantity of catalyst again the autoclave was charged with pretreated catalyst and reactants as per above-mentioned method.

3 Result and Discussion

Synthetic hydrotalcite was prepared via well-reported coprecipitation method using $Mg(NO_3)_2$ and $Al(NO_3)_2$, under basic condition. The corresponding white precipitates were dried at 110 °C and further calcined at 600 °C for 4 h. The alkoxysilane containing bidentate iminophosphine ligand [*o*-$Ph_2PC_6H_4CH{=}N(CH_2)_3Si(OMe)_3$] **A** was synthesized by reacting 2-(Diphenylphosphino) benzaldehyde with 3-(Trimethoxysilyl)propylamine under a nitrogen atmosphere in dry THF. All the analytical data obtained from NMR analysis ($^1H/^{13}C/^{31}P$) were found in agreement with the reported data for the same [18]. Again, iminophosphine ligand **A** was grafted on the surface of calcined hydrotalcite material by refluxing the reaction mass in dry toluene for 24 h. Unreacted or loosely coordinated iminophosphine ligand **A** was isolated by Soxhlet extraction method. The resulting solid material was dried under vacuum at 100 °C to obtain ABIL-HT-A (Fig. 1). At last, ABIL-HT-A went to metalation step. The resulting HRUC-A material was obtained in the black color solid and properly stored in an argon atmosphere. In addition, we synthesized a series of hydrotalcite anchored monodentate phosphine based materials such as HRUC-B, HRUC-C and HRUC-D using ABIL-HT-B, ABIL-HT-C and ABIL-HT-D respectively (Fig. 1). We also created iminophosphine ligand without out alkoxysilane moiety **A** to use them as a reference material to understand the physiochemical properties of our developed materials (Fig. 2).

We used various sophisticated techniques to understand the physiochemical properties of HRUC materials (Figs. 2, 3) like ^{13}C & ^{29}Si NMR, DRIFT, FTIR, XPS, elemental analysis using AAS, BET surface analysis and inductively coupled plasma optical emission spectroscopy (ICP-OES).

Solid state ^{13}C & ^{29}Si NMR analysis were applied to understand the surface structure of functionalized hydrotalcite materials (Figs. 3, 4a, b). This analysis helps to know the structure and bonding of hydrotalcite with alkoxysilane moiety. The ^{13}C NMR spectrum of an organic moiety of HRUC-A confirmed that bidentate iminophosphine ligand is properly intact with hydrotalcite support. This was also confirmed by the report published by Wang et al. [19]. No peak corresponding to the methoxy group of trimethoxysilane was found in ^{13}C NMR analysis which also supports that all the three methoxy groups have been lost during functionalization of hydrotalcite as HRUC-A. This data confirms the tripodal (T^3) type arrangement of silane moiety over hydrotalcite. ^{29}Si NMR analysis provided the insight nature of M–O–Si bonds on the hydrotalcite surface. The two distinct peaks confirmed in ^{29}Si NMR confirmed the anchoring of silane groups to Mg_3-OH and $AlMg_2$-OH environment respectively. Almost similar results were observed in other HRUC-B to D materials.

We performed diffuse reflectance infrared Fourier transform spectroscopy (DRIFTS) (is an infrared spectroscopy

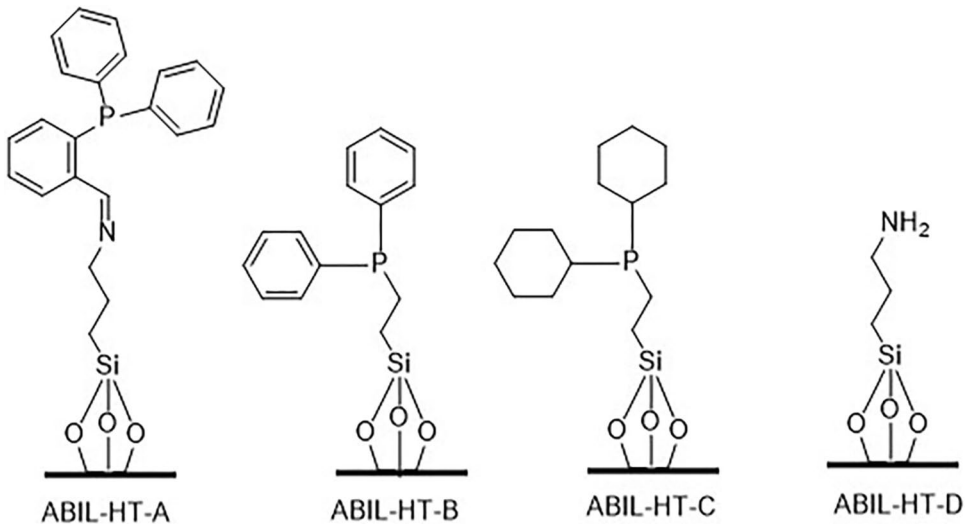

Fig. 1 Hydrotalcite supported phosphine ligands

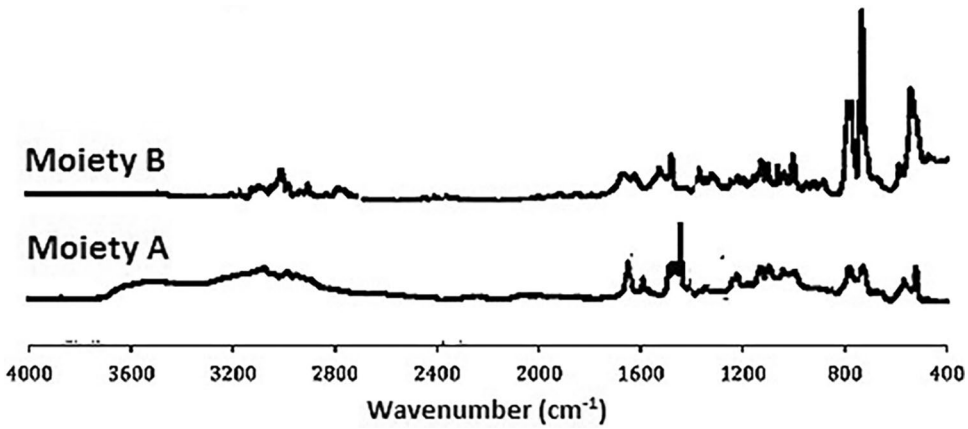

Fig. 2 DRIFT analysis data for Moiety A and B

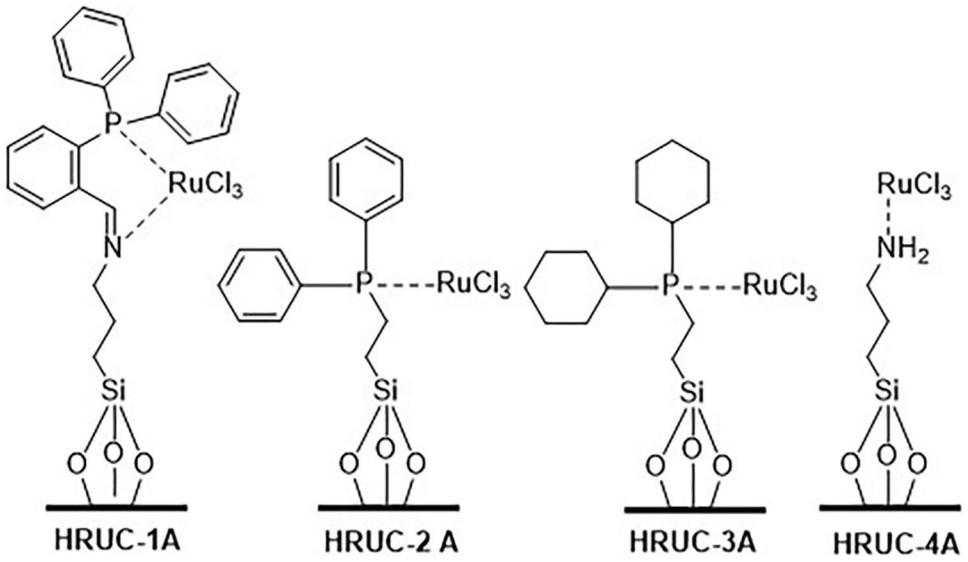

Fig. 3 Hydrotalcite supported ruthenium catalyst

technique) for iminophosphine ligand (without alkoxysilane) and iminophosphine ligand with alkoxysilane moiety. Collectively, we used this data to understand the structure of HRUC-A to D. We located the position of Schiff base (CH=NR) double bond near to 1640 cm^{-1}. The vibrations peaks of phenyl rings in HRUC-A and B materials located on following regions 3061, 1580, 1430, 741 and 694 cm^{-1}. The similar peaks for phenyl rings were observed in ABIL-HT-A and ABIL-HT-B. Such data confirms the presence of Schiff base before and after the metalation of our developed materials. In FTIR analysis, we also recorded different types of absorption peaks for HRUC-A to D (Figs. 5, 6).

Before going to the metalation step, we performed surface analysis using N_2-physisorption analysis for hydrotalcite (before and after calcination) and after the functionalization calcined hydrotalcite clay. All the data were tabulated and Table 3. A noticeable increase in the BET surface area, pore size, and pore (single point pore volume measured at $P/P_o = 0.97$ on absorption) volume were recorded in calcined hydrotalcite material with respect to normal hydrotalcite material. A visible drop in terms of the BET surface area, pore size and pore volume were found in functionalized calcined hydrotalcite materials (ABIL-HT-A to D). The lowest value of BET surface area, pore size, and pore volume noted for ABIL-HT-B. After completion of metalation process for ABIL-HT-A to D materials, we also checked the BET surface area, pore size and pore volume along with elemental analysis. This data helped us to understand the metallic composition of both ABIL-HT-A to D and HRUC-A to D materials (Table 3). Considering the matrix effect, we performed the elemental analysis using AAS method to confirm the quantity of Mg, Al, Si and Ru contents in our developed materials. The silica content was only recorded in functionalized hydrotalcite clay, in the same pattern Ru metal signal was only logged for HRUC-A to D materials. Slightly, a higher amount of Ru metal was found in HRUC-A material with respect to other HRUC-B to D materials.

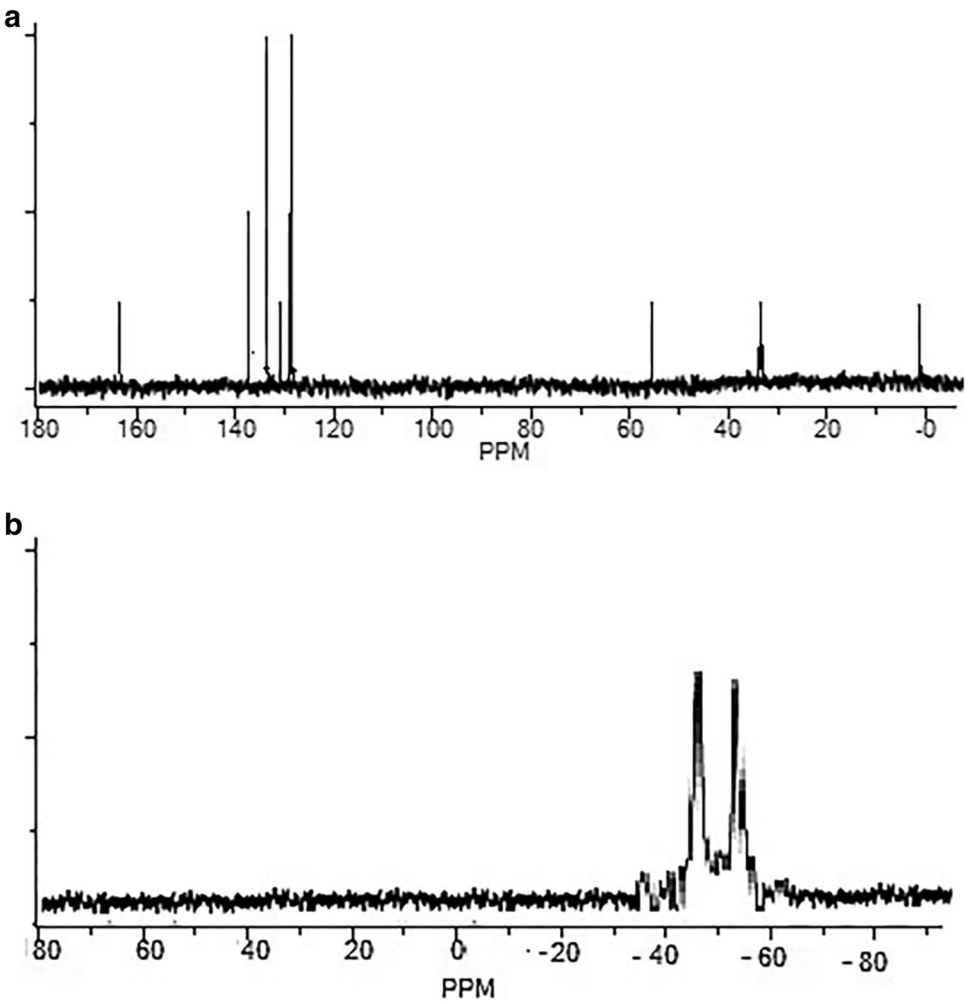

Fig. 4 **a** ^{13}C analysis of HRUC-A (except solvent peak). **b** ^{29}Si analysis of HRUC-A material

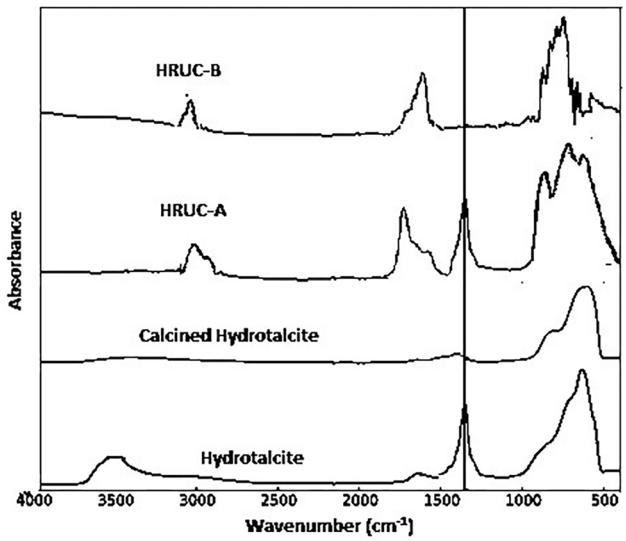

Fig. 5 DRIFT analysis data of HRUC-A, ABIL-HT-A and hydrotalcite

XPS analysis was performed to understand the composition of different HRUC-A to D materials. The Ru 3d, C1, N 1S and P 2p levels were calculated at a normal angle with respect to the plane of the surface during XPS spectra calculation. Binding energy was carefully measured with a precision of ± 0.2 eV. Shirley background subtraction, as well as Gaussian and Lorentzian principal for peak shape, was considered while doing XPS analysis of Ru 3d levels. The peaks near to 280.2 eV (Ru $3d_{5/2}$) and 284.3 eV (Ru $3d_{3/2}$) inveterate the attendance of Ru (0) species. Unexpectedly, no signs of RuO_2 were recorded while performing the XPS analysis of HRUC-A to D materials. This observation was also supported as no peak was found to represent Ru 3p with binding energy 464 eV which confirmed the absence of Ru species with +2 oxidation state. We also linked the XPS data of $RuCl_3$/calcined hydrotalcite material with XPS data of HRUC-A to D materials and intimated the occurrence of Ru (0) species (Table 4).

Some resemblance with respect to Ru $3d_{5/2}$ and Ru $3d_{3/2}$ were found between HURC-B and $RuCl_3$/Calcined hydrotalcite materials which established the low loading

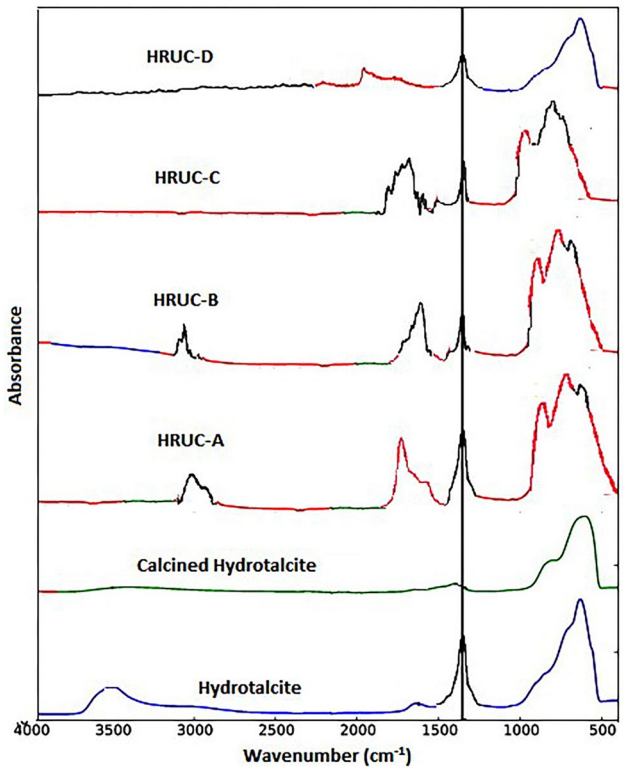

Fig. 6 DRIFT analysis data for HRUC-A to D and Hydrotalcite

of phosphine ligands on support. In contrast, much higher phosphine loading was recorded in HRUC-C, which resulted in a higher binding energy for Ru $3d_{5/2}$ and Ru $3d_{3/2}$. The binding energies of HRUC-A for Ru $3d_{5/2}$ and Ru $3d_{3/2}$ were found almost like Ru-PNPr[1]. These results signpost that the location of Ru metal in HRUC-A is identical to Ru-PNPr[1] species. TEM data also used to confirm the morphology of the Ru metal loaded functionalized hydrotalcite material (Fig. 7). TEM image of all the HRUC-A to D materials along with hydrotalcite and calcined hydrotalcite materials were recorded. The image analysis of HRUC-A to D materials inveterate the presence of well dispersed Ru nanometal in the range of 8–10 nm (± 0.25) with a mean diameter of 4.5 nm. TEM image analysis also disclosed the presence of highly crystalline nature of Ru nanometals.

3.1 Hydrogenation of CO_2 to Formic Acid Without Ionic Liquid Medium

Formic acid is one of the important chemicals in organic chemistry. It has been reported as a starting chemical for the synthesis of a large variety of beneficial chemical derivatives such as aldehydes, ketones, amine and carboxylic acid. It also utilized in the manufacturing of perfume and fragrance [1]. Transition metal complex catalysts were widely applied to utilize CO_2 gas as a C1 synthetic unit in formic acid synthesis. Although this developed catalytic system offers the production of formic acid, these catalytic protocols also suffer from the selectivity and low reactivity of CO_2 gas due to its high thermodynamic stability ($+\Delta G^{\circ}_{298} = 32.9$ KJ/mol). Considering the above-mentioned facts, we tested our developed catalytic systems (HRUC-A to D) for the selective hydrogenation of CO_2 to formic acid under high-pressure reaction condition in presence of triethylamine and a small quantity of water at 80 °C. We used cyclohexanone as an internal standard in the reaction mass.

All results obtained while using HRUC-A to D catalysts were tabulated in Table 1, entry 1–18, Scheme 1. The quantity of formic acid was calculated using ^{1}H NMR and acid-base titration (Fig. 8). Dioxane was added in the reaction mass before starting the reaction as an internal standard. After completion of the reaction, a small quantity of reaction mass was used for 1H NMR analysis, which confirms the formation of formic acid along with no formation of any side product during the reaction. The quantity of formic acid calculated via ^{1} H NMR was found in good agreement with the data obtained from acid-base titration of reaction mass.

Table 3 Physiochemical analysis of synthesized materials

S. no.	Sample	Mg%	Al%	Si%	Ru%	S_{BET} (m^2/g)	Pore volume (cm^3/g)	Pore size (nm)	Particle size of Ru nanometal
1.	Hydrotalcite	26.3	11.9	–	–	110	0.31	7.1	–
2.	Hydrotalcite-clacined	38.8	11.2	–	–	119	0.39	7.8	–
3.	ABIL-HT-A	38.1	11.1	–	–	108	0.34	7.2	–
4.	ABIL-HT-B	36.9	10.9	–	–	76	0.23	6.7	–
5.	ABIL-HT-C	36.9	10.8	–	–	98	0.29	6.1	–
6.	ABIL-HT-D	37.7	9.9	–	–	81	0.27	6.4	–
7.	HRUC-A	37.9	10.9	8.98	3.2	106	0.32	7.1	8
8.	HRUC-B	36.2	10.5	8.69	2.1	75	0.21	6.5	10
9.	HRUC-C	36.4	10.8	8.71	2.3	93	0.28	6	9.3
10.	HRUC-D	37.1	10.8	8.72	2.9	80	0.25	6.2	8.7

Table 4 XPS analysis of different developed materials

Samples[a,b]	Ru $3d_{3/2}$ [eV]	Ru $3d_{5/2}$ [eV]	Cl_2 2p [eV]	P 2p [eV]	N 1s [eV]
$RuCl_3$	284.6	280.2	199.2	–	–
$RuCl_3$/calcined hydrotalcite	284.4	280.1	199.1	–	–
Ru-PNPr[1]	284.7	280.8	198.6	131.9	399.8
ABIL-HT-A	–	–		131.8	398.1
ABIL-HT-B	–	–	–	–	–
ABIL-HT-C	–	–	–	131.1	–
ABIL-HT-D	–	–	–	131.1	–
HRUC-A	284.7	280.8	197.1	131.8	400.1
HRUC-B	284.7	284.8	198.6	131.7	–
HRUC-C	284.6	284.5	199.3	131.6	–
HRUC-D	284.6	284.5	199.3		400.2
HRUC-A (*after catalyst recycling*)	284.6	284.4	198.5	131.6	–

[a]Measurement error of ± 0.2 eV; XPS data of Si 2p at 103.3 eV

[b]XPS data referenced to C 1s at 284.5 eV

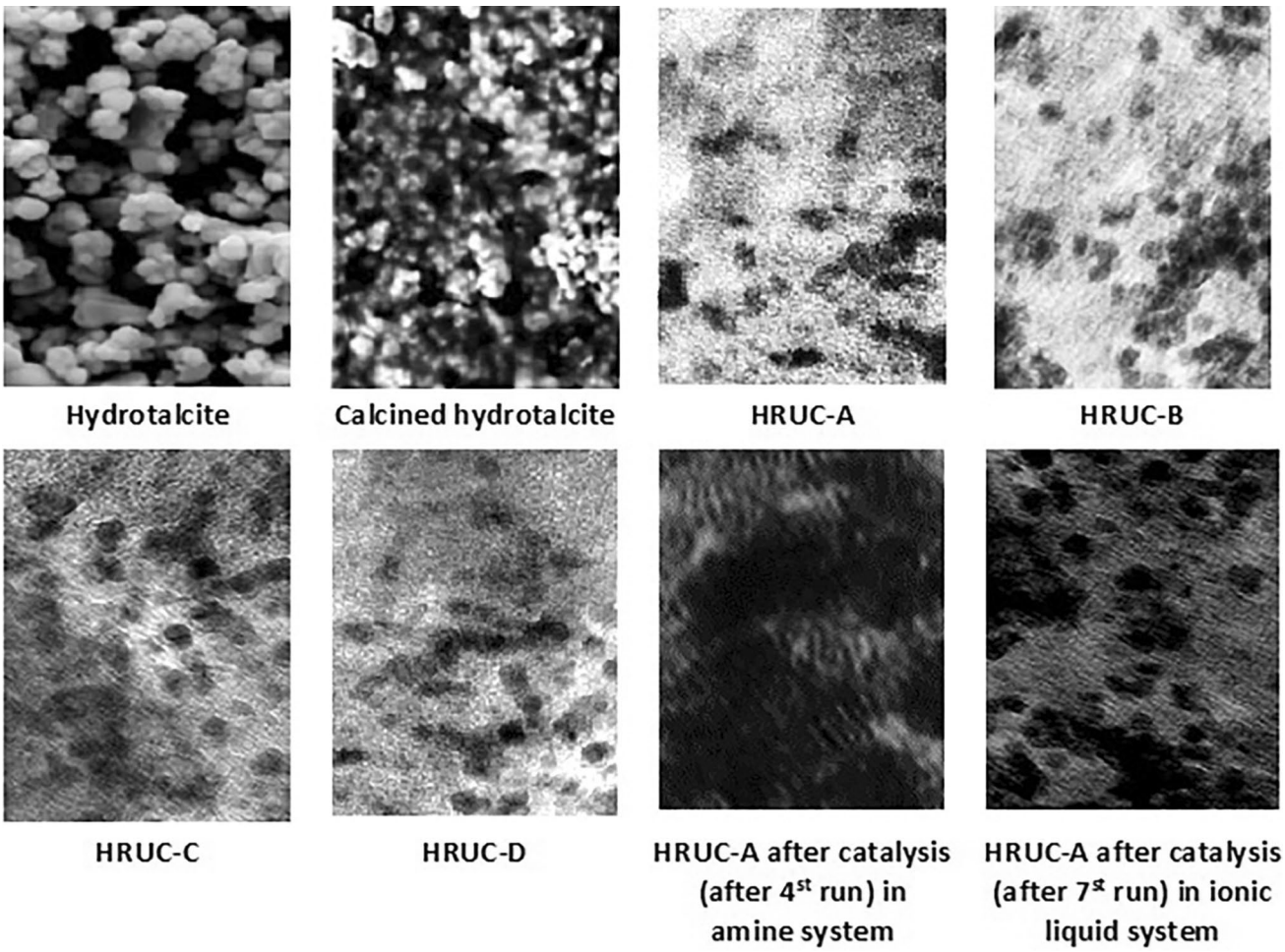

Fig. 7 TEM images of all HRUC catalysts

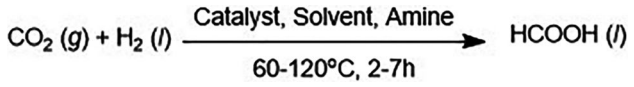

Scheme 1 CO_2 hydrogenation in triethylamine

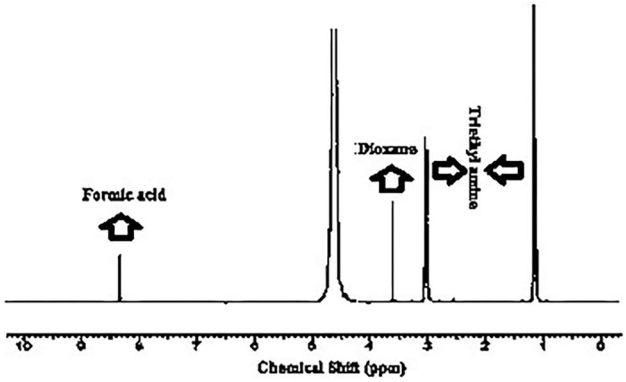

Fig. 8 ^{1}H NMR analysis after hydrogenation of CO_2

A small quantity of formic acid was reported in absence of triethylamine which confirmed that the basic nature of hydrotalcite clay also influences the hydrogenation of CO_2 gas up to certain extent. $RuCl_3{\cdot}3H_2O$ precursor, as well as $RuCl_3$, supported calcined hydrotalcite material gave formic acid with a low TON and TOF values. Low quantity of formic acid was recorded with amine functionalized HRUC-D catalysts with respect to phosphine functionalized HRUC-A to C catalytic system. This observation confirmed the high activity of phosphine functionalized HRUC-A to C catalytic systems for the hydrogenation of CO_2 gas. The bidentate phosphine functionalized HRUC-A catalyst gave formic acid with a high TON and TOF value with respect to other catalytic systems (HRUC-B to D). We performed all the optimization step with HRUC-A catalyst to get a high quantity of formic acid. Changing the temperature, reaction time, quantity of reactant/catalyst quantity gave a noticeable change in formic acid production. Ru metal loaded moiety-A gave the lowest value of formic acid due to the Ru–Ru metal dimerization in the reaction solution.

Filtration test was performed to know the stability of HRUC-A to D catalytic systems. After completion of hydrogenation reaction under optimized reaction condition (Table 1, entry 4), the solid part of the reaction was isolated through 0.45 nm polytetrafluoroethylene (PTFE) filter and the filtered was used to perform the hydrogenation reaction. We found a small quantity of formic acid with TOF value of 12 h^{-1}. This test confirmed the catalytic leaching during the reaction which was further supported by XPX and ICP-OES analysis of Ru metal infiltrate. The same observation was observed while recycling the HRUC-A catalyst. We only recorder the recycling test up to four cycles mainly because of catalysts leaching as well as Ru metal agglomeration (Fig. 7). The size of Ru metal was increased from 8 to 78 nm (Fig. 9).

3.2 Hydrogenation of CO_2 to formic acid with ionic liquid medium

May attractive properties of ionic liquids like extremely low volatility, high thermal stability, strong solvation nature for various substances and wide liquid-temperature range makes them promising alternative solvent over conventional solvent systems. Additionally, functionalized ionic liquid (by changing the anion or cation or grafting functional group on to ions) extended the application ionic liquids in catalysis, extraction, absorption of gases such as CO_2, H_2, SO_2 etc.

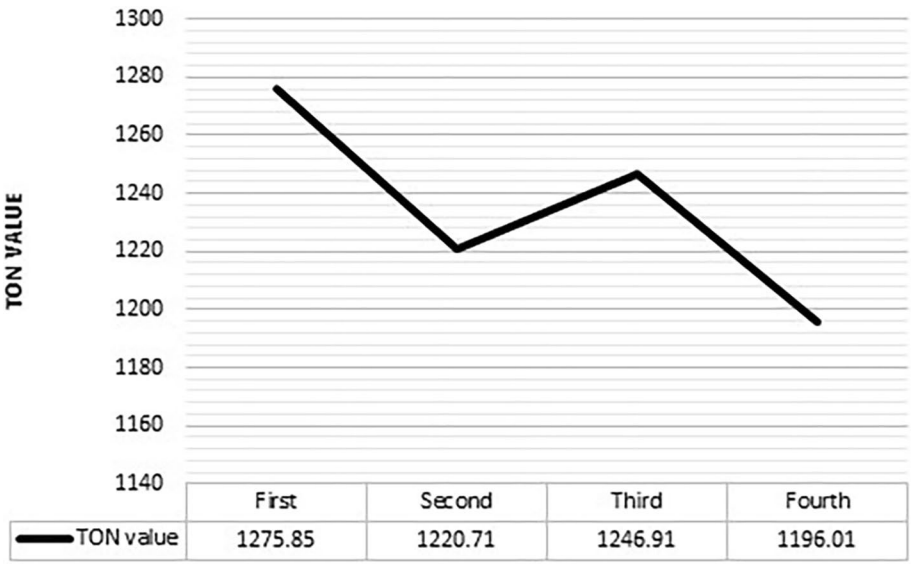

Fig. 9 HRUC-A catalyst test result data

In our previous studies, we synthesized a series of functionalized ionic liquid liquids such as like 1-(*N,N*-dimethylaminoethyl) 2,3-dimethylimidazolium trifluoromethanesulfonate ([mammim][TfO]), and 1,3-*di*(*N,N*-dimethylaminoethyl)-2-methylimidazolium *bis* (trifluoromethylsulfonyl) imide ([DAMI][NTf_2])were synthesized as per the reported procedures while ionic liquids such as 1-(*N,N*-dimethylaminoethyl) 2,3-dimethylimidazolium *bis* (trifluoromethylsulfonyl) imide ([mammim][NTf_2]), 1-(*N,N*-dimethylaminoethyl)-2,3-dimethylimidazolium nonafluorobutanesulfonate ([mammim][$CF_3CF_2CF_2CF_2SO_3$]), 1-(*N,N*-dimethylaminoethyl)-2,3-dimethylimidazolium trifluoromethanesulfonate ([mammim] [BF_4]), 1,3-*di*(*N,N*-dimethylaminoethyl)-2-methylimidazolium trifluoromethanesulfonate ([DAMI][TfO]), 1,3-*di*(*N,N*-dimethylaminoethyl)-2-methylimidazolium nonafluorobutanesulfonate ([DAMI][$CF_3CF_2CF_2CF_2SO_3$]) and 1,3-*di*(*N,N*-dimethylaminoethyl)-2-methylimidazolium tetrafluoroborate ([DAMI][BF_4]) in order to obtained high degree of chemo selectivity, easy catalyst recycling and informal product isolation [4, 5, 20–22]. Moreover, we also did a comprehensive study on the absorption of CO_2 gas in above mentioned functionalized ionic liquid. In our study, we found 1,3-*di*(*N,N*-dimethylaminoethyl)-2-methylimidazolium nonafluorobutanesulfonate ([DAMI][$CF_3CF_2CF_2CF_2SO_3$]) ionic liquid as an promising reaction medium [5, 20–22]. The above observation supports the CO_2 solubility in ionic liquids mainly depends on the presence of branched chains or polar groups and CO_2-philic groups in the anionic or cationic parts of the ionic liquid structure. Such modifications in ionic liquid morphology increase the free volume to accommodate CO_2 gas [4, 20]. In addition, the physiochemical property of anions of ionic liquid plays a significant role in the solubility of CO_2 gas than the cations. Ionic liquid, carrying highly fluorinated anions were recorded to have the highest CO_2 solubility among the ionic liquids with the same cations. Apart from such advantages, C–F bond of anions increases the rigidity and decreases the polarity of ionic liquid. Such change in the properties of ionic liquid, not only leads to higher gas solubility in highly fluorinated as well as sulfonated ionic liquids, but also makes easier the regeneration of the ionic liquid [4, 5, 20–22].

The density of this ionic liquid was measured by using capillary pycnometer and found 1.235 g/mL. We also calculated the glass transition temperature of this ionic liquid using differential scanning calorimetry and recorded to be − 41 °C. This ionic liquid was also analyzed by means of thermogravimetric analysis which indicates that the ionic liquid is found stable up to 225 °C (Fig. 10).

In this manuscript, we took this ionic liquid as a reaction medium to perform the CO_2 hydrogenation using HRUC-A catalyst. All the experimental results of CO_2 hydrogenation reaction are represented in Table 2, entry 1–18, Scheme 2.

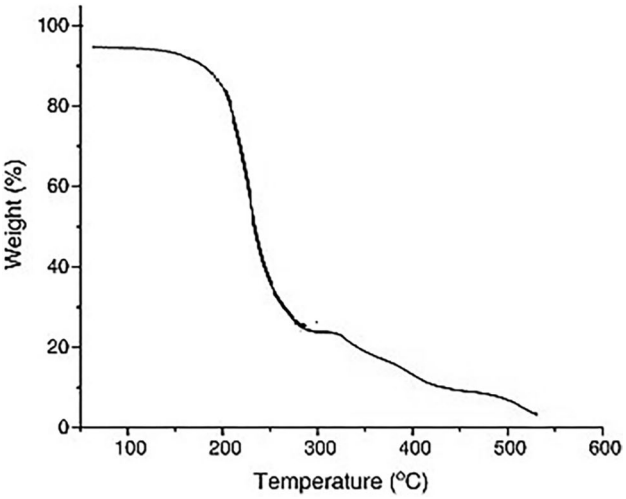

Fig. 10 TGA analysis data of [DAMI][$CF_3CF_2CF_2CF_2SO_3$] ionic liquid

Heterogenous nature of HRUC-A catalyst in ([DAMI][$CF_3CF_2CF_2CF_2SO_3$]) ionic liquid was investigated as per the reported procedure of *catalyst poisoning experiments* [23]. The above-mentioned protocol was found relatively simple and both ionic liquid as well catalyst was recycled straightforwardly. It is also expected that the competence of the HRUC-A catalyst was increased due to the presence of two -NH functional groups on both the ends of the ionic liquid. The synergic effect of ionic liquid with HRUC-A catalysts was also studied and it was found while using [bmim][NTf_2] ionic liquid (as nonfunctional ionic liquid) with HRUC-A catalyst, formic acid was obtained with low TON/TOF value (Table 2, entry 16).

After completion of CO_2 hydrogenation, the reaction mass was heated to isolate first water and then formic acid with help of N_2 flow. The presence of a base (ionic liquid and hydrotalcite material) and formic acid in the reaction mass developed an equilibrium between free formic acid, formic acid salt, ionic liquid and hydrotalcite material. The amount of free formic acid was increased with increasing the temperature as the acid-base neutralization to salt is an exothermic process. Considering the fact, separation of formic acid was carried out under nitrogen flow at optimized temperature.

All the CO_2 hydrogenation results were tabulated in Table 2 and Scheme 2. Surprisingly no by-product was reported during hydrogenation reaction (confirmed by ^1H NMR). We started our study with changing the molar ratio of formic acid/HRUC-A + ionic liquid at 80 °C and 20 MPa as a function of time is represented in Fig. 3. The almost linear increase was found between formic acid/HRUC-A + ionic liquid ratio near to 1:81 at 5 h. After this time no, drastic change in ratio was reported but while increasing the

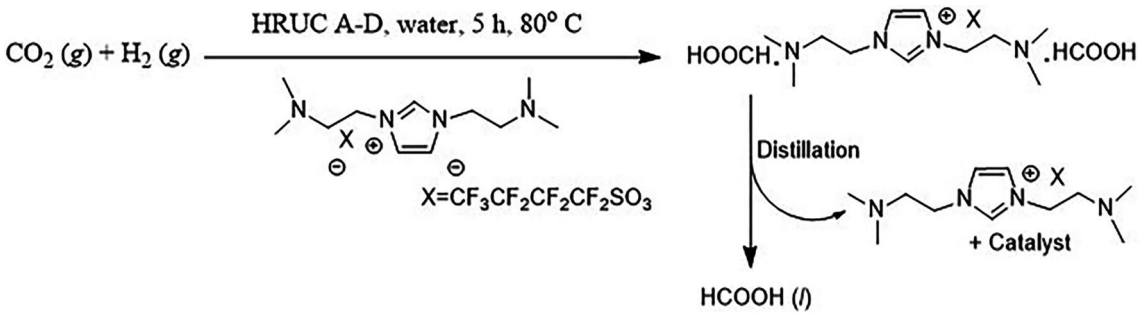

Scheme 2 CO_2 hydrogenation reaction in ionic liquid medium

temperature and after 6 h the ration between formic acid/HRUC-A + ionic liquid was found equal to 2.1 at 6–10 h. This observation showed that free formic acid combined with the basic HRUC-A + ionic liquid system and formed the formic acid salt. In starting, formic acid neutralization was fast with respect to the formic acid formation. At high ratio on formic acid/ionic liquid, most of the ionic liquid got neutralized but HRUC-A + ionic liquid system and formic acid produced remained same in the system.

The effect of water was also evaluated (Table 2, entry 1–7). It was clearly observed in our study that TON–TOF value of formic acid was increased by adding water. This increase can be explained in two different manners. First, the addition of water will reduce the viscosity of the ionic liquid and second, presence water may increase the chances of bicarbonate formation due to the reaction of the CO_2 gas with water and basic ionic liquid system. In some of the reports, these bicarbonate species are treated as the true substrate for hydrogenation reaction (Fig. 11).

The hydrogenation reaction was carried out at different temperature and reaction pressure and time (Table 2, entry 14). On increasing the temperature rate of reaction got increased and the TON value of formic acid was increased up to 1581.62 at 100 °C (Table 2, entry 7 and 8). As pressure increased from 20 to 30 MPa at 80 °C, TON and TOF value were also found higher and recorded 1886.94 and 317.4 respectively. The pressure effect in this reaction can be explained according to Henry's law, as the solubility of two gases increases along with increasing the pressure, because of that concentration of reactants have great importance on the rate of reaction [4, 5, 20–22].

We recovered the formic acid followed by distillation process under nitrogen flow. No sign of ionic liquid decomposing and side product formation was recorded during the reaction. This observation was supported by ^{1}HNMR analysis of crude reaction mass. We used simple titration method as well as ^{1}HNMR analysis to quantify the amount of formic acid. Data from both analysis found in good agreement.

To understand the stability of [DAMI][$CF_3CF_2CF_2CF_2SO_3$]/HRUC-A catalytic system we performed the

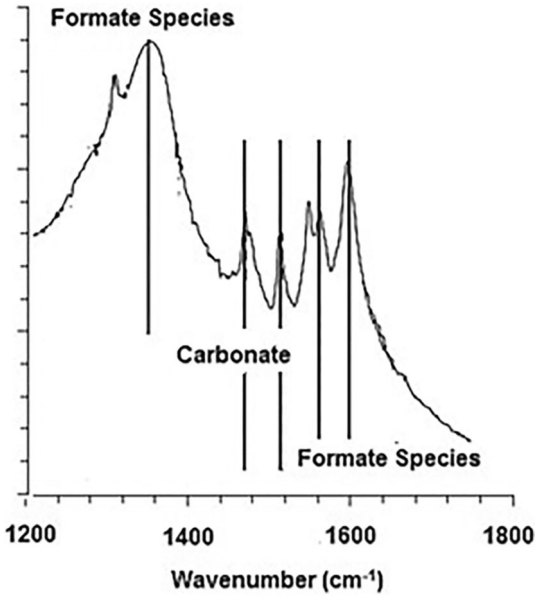

Fig. 11 FTIR data of format and carbonate species formed during the reaction

filtration experiment. In this experiment, we mixed our catalytic system with 10 mL of water and heated the resulting mixture at 80 °C for next 6 h under 40 bar hydrogen pressure in an autoclave. After cooling the reaction mass and degassing the autoclave the resulting mixture was filtered, and the filtrate was used to for the CO_2 hydrogenation experiment. Surprisingly, no sign of formic acid was found. This result was also supported by ICP-OES and XPS method that no Ru metal was detected in the solution.

Taking the advantage of above experimental results, we exploited our catalytic system for catalyst recycling test. After completion the reaction, the reaction product was isolated, and the complete catalytic system was recycled to next run (after pretreatment process). We easily recycled our catalytic system up to eight runs (Fig. 12). The drop-in catalyst activity was recorded after 8th run mainly

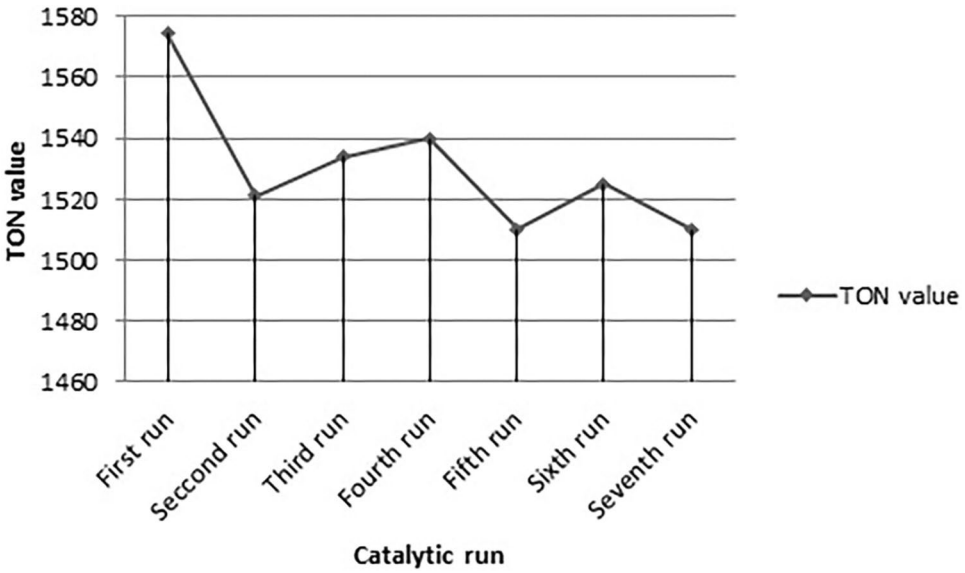

Fig. 12 [DAMI][$CF_3CF_2CF_2CF_2SO_3$]/HRUC-A catalyst recycling

due to agglomeration of Ru metal as the size of metal was increased from 8 to 34 nm (TEM image, Fig. 7).

After combing the outcomes of all characterization and conclusions of available scientific reports [24, 25], we can suggest a conceivable catalytic procedure for CO_2 hydrogenation over HRUC-A (Schiff base Ru catalysts) in diamine based [DAMI][$CF_3CF_2CF_2CF_2SO_3$] ionic liquid. CO_2 molecule was captured by the damine functionalized ionic liquid through a carbamate zwitterion intermediate, which also served as a reservoir for CO_2 in the liquid phase. This weakly chemisorbed CO_2 could migrate and interacted to the Ru–Schiff base interface without losing its carbamate zwitterion nature [26, 27]. At the same time, the low-coordinated sites of the Ru nanoclusters also participated in the activation and dissociation of H_2 to the activated H species. Then, the carbamate zwitterion intermediates were hydrogenated by the H species at the Ru–Schiff base interface, and the formate was thus obtained after a two-step hydrogenation and acid–base neutralization in an alkaline environment. Notably, the electron-rich Ru surface, caused by the electron donation from nitrogen groups, might also be beneficial for the hydrogenation of CO_2, since it could offer a more negative hydride and lead to a higher reactivity of the nucleophilic attack to the carbon center of CO_2 [27].

4 Conclusion

In summary, we synthesized a series of active hydrotalcite supported Ru metal complexes (HRUC-A to D) to catalyze hydrogenation of CO_2 gas with and without ionic liquids. HRUC-A catalyst was found highly active and gave good quantity of formic acid. The combination of basic ionic liquid [DAMI][$CF_3CF_2CF_2CF_2SO_3$] with HRUC-A catalytic was found extremely efficient to get formic acid with high TON and TOF value. In our study we found that the CO_2 molecule is activated due to the formation of a weak carbamate zwitterionic intermediate at the Ru–Schiff base interface in HRUC-A. This step plays an important role afterward it provides the development of formate species. Furthermore, the catalytic pathway is also benefited due to the presence of amine group of ionic liquid ([DAMI][$CF_3CF_2CF_2CF_2SO_3$]), which permits the creation of a reservoir of CO_2 by capturing the gaseous CO_2 through the same type of zwitterion intermediate. The Schiff-base-modified Ru nanocatalyst (HRUC-A) displayed a rare catalytic performance compared other reported hydrotalcite supported Ru metal complexes and shows excellent activity toward CO_2 hydrogenation to formic acid formation. The addition of water and increase in pressure as well as temperature resulted high reaction rate [28]. The molar ration of formic acid to ionic liquid was reached up to 2.1 (0.276:1 w/w) in one reaction cycle. The recovery of formic acid from the reaction mass was very easy and [DAMI][$CF_3CF_2CF_2CF_2SO_3$]/HRUC-A catalytic system was found recyclable up to eight runs. A drastic effect of ionic liquid was recorded over the stability (*in terms of catalyst leaching*) HRUC-A catalyst. Without ionic liquid HRUC-A catalyst was recycled only up to four cycles. This simple, efficient, and green protocol to get formic acid is economical, energy efficient and has potential to be applied in industry.

Compliance with Ethical Standards

Conflict of interest The authors declare no conflict of interest.

References

1. Upadhyay P, Srivastava V (2016) Carbon sequestration: hydrogenation of CO_2 to formic acid. Present Environ Sustain Dev 10(2):13–34
2. Keeling RF (2009) Triage in the greenhouse. Nat Geosci 2(12):820–822
3. Le Quéré C, Raupach MR, Canadell JG, Marland G (2009) Trends in the sources and sinks of carbon dioxide. Nat Geosci 2(12):831–836
4. Upadhyay PR, Srivastava V (2016) Titanium dioxide supported ruthenium nanoparticles for carbon sequestration reaction. Nanosyst: Phys Chem Math 7(3):513–517
5. Upadhyay P, Srivastava V (2016) Synthesis of monometallic Ru/TiO_2 catalysts and selective hydrogenation of CO_2 to formic acid in ionic liquid. Catal Lett 146(1):12–21
6. Saeidi S, Amin NAS, Rahimpour MR (2014) Hydrogenation of CO_2 to value-added products—a review and potential future developments. J CO2 Util 5:66–81
7. Wang W, Wang S, Ma X, Gong J (2011) Recent advances in catalytic hydrogenation of carbon dioxide. Chem Soc Rev 40(7):3703–3727
8. Álvarez A, Bansode A, Urakawa A et al (2017) Challenges in the greener production of formates/formic acid, methanol, and DME by heterogeneously catalyzed CO_2 hydrogenation processes. Chem Rev 117(14):9804–9838
9. Wiyantoko B, Kurniawati P, Purbaningtias TE, Fatimah I (2015) Synthesis and characterization of hydrotalcite at different Mg/Al molar ratios. Proced Chem 17:21–26
10. Sikander U, Sufian S, Salam MA (2016) Synthesis and structural analysis of double layered Ni-Mg-Al hydrotalcite like catalyst. Proced Eng 148:261–267
11. Nalawade P, Aware B, Kadam VJ, Hirlekar R (2009) Layered double hydroxides: a review. J Sci Ind Res 68(4):267–272
12. Saifullah B, Hussein MZB (2015) Inorganic nanolayers: structure, preparation, and biomedical applications. Int J Nanomed 10:5609–5633
13. Srivastava V (2013) Recyclable hydrotalcite clay catalysed Baylis-Hillman reaction. J Chem Sci 125(5):1207–1212
14. Upadhyay PR, Srivastava V. Clays (2016) An encouraging catalytic support. Curr Catal 5(3):162–181
15. Lakshmi Kantam M, Vijaya Kumar K, Sreedhar B (2007) Asymmetric hydrogenation of ethyl pyruvate using layered double hydroxides–supported nano noble metal catalysts. Synth Commun 37(6):959–964
16. Baskaran T, Christopher J, Sakthivel A (2015) Progress on layered hydrotalcite (HT) materials as potential support and catalytic materials. RSC Adv 5(120):98853–98875
17. Liu Y, Yu T, Cai R, Li Y et al (2015) One-pot synthesis of NiAl-CO_3 LDH anti-corrosion coatings from CO_2-saturated precursors. RSC Adv 5(37):29552–29557
18. Finn M, An N, Voutchkova-Kostal A (2015) Immobilization of imidazolium ionic liquids on hydrotalcites using silane linkers: retardation of memory effect. RSC Adv 5(17):13016–13020
19. Yang H, Han X, Li G, Wang Y (2009) N-Heterocyclic carbene palladium complex supported on ionic liquid-modified SBA-16: an efficient and highly recyclable catalyst for the Suzuki and Heck reactions. Green Chem 11(8):1184–1193
20. Upadhyay PR, Srivastava V (2016) Selective hydrogenation of CO_2 using ruthenium nanoparticles intercalated montmorillonite clay. Lett Org Chem 13(6):459–465
21. Upadhyay PR, Srivastava V (2016) Selective hydrogenation of CO_2 gas to formic acid over nanostructured Ru-TiO_2 catalysts. RSC Adv 6(48):42297–42306
22. Srivastava V (2014) Ru-exchanged MMT clay with functionalized ionic liquid for selective hydrogenation of CO_2 to formic acid. Catal Lett 144(12):2221–2226
23. Alonso F, Riente P, Sirvent JA, Yus M (2010) Nickel nanoparticles in hydrogen-transfer reductions: characterisation and nature of the catalyst. Appl Catal A 378(1):42–51
24. Hao C, Wang S, Li M, Kang L, Ma X (2011) Hydrogenation of CO_2 to formic acid on supported ruthenium catalysts. Catal Today 160:184–190
25. Gunasekar GH, Park K, Jung KD, Yoon S (2016) Recent developments in the catalytic hydrogenation of CO_2 to formic acid/formate using heterogeneous catalysts. Inorg Chem Front 3:882–895
26. Wang YB, Wang YM, Zhang WZ, Lu XB (2013) Fast CO_2 sequestration, activation, and catalytic transformation using N-heterocyclic olefins. J Am Chem Soc 135:11996–12003
27. Villiers C, Dognon JP, Pollet R, Thuéry P, Ephritikhine M (2010) An isolated CO_2 adduct of a nitrogen base: crystal and electronic structures. Angew Chem Int Ed 49:3465–3468
28. Qinggang L, Xiaofeng Y, Lin L, Shu M, Yong L, Yanqin L, Xinkui W, Yanqiang H, Tao Z (2017) Direct catalytic hydrogenation of CO_2 to formate over a Schiff-base-mediated gold nanocatalyst. Nature Commun 8:1–8